

Phase-matched second-harmonic generation by periodic poling of fused silica

Raman Kashyap, Gerrit J. Veldhuis,^{a)} David C. Rogers, and Paul F. Mckee
BT Laboratories, Martlesham Heath, Ipswich IP5 7RE, United Kingdom

(Received 22 September 1993; accepted for publication 15 December 1993)

90° phase matching in periodically poled fused silica is achieved over approximately 2 mm at a wavelength of 1064 nm. Electrical poling was done at 5 kV for 120 min using photolithographed periodic electrodes on fused silica glass at 250 °C. A nonlinearity equivalent to $d_{11}/200$ of quartz is estimated from measurements. Several phase-matched interactions are reported and the implications for device applications discussed.

Electrical poling of silica at high temperature to induce a nonlinearity of 1 pm V⁻¹ in a thin layer below the surface of the positive electrode is a recently reported intriguing phenomenon.^{1,2} It has been proposed from available data that migration of sodium ions through the substrate, rather than electrons (due to the low electronic conductivity in silica) causes a space-charge field to develop in a depleted region some micrometers below the surface of the positive electrode.

Recently, it has been demonstrated that *e*-beam exposure may also be used to induce a similar nonlinearity.³ The observations indicate that the nonlinearity is anonymously large and beg the question of whether or not a periodic nonlinearity may be induced for efficient nonlinear interactions. Owing to the spreading of the electric field below the positive electrode in the case of simple electrical poling and surface charging in the case of *e*-beam poling, there is some question as to whether or not a small enough feature can be written directly into glass to create a periodic nonlinearity. In this letter it is demonstrated that direct periodic electrical poling is possible to achieve phase-matched second harmonic generation from 1064 nm radiation in several samples of fused silica. Various regimes are investigated to achieve 90° broadband phase matching as well as shallower angle narrow bandwidth frequency doubling.

First of all 6-mm-thick samples of fused silica were poled by subjecting them to 5 kV at 250 °C for 120 min. Samples were then probed for second-harmonic generations (SHG) by propagation of 1064 nm *Q*-switched Nd:YAG laser light focussed with a 400 nm focal length lens in the poling direction. The same was rotated to observe SHG as in Maker-fringe analysis⁴ (see inset Fig. 1). The output is shown in Fig. 1. The asymmetry is due to aperturing at the input of the photomultiplier tube owing to beam deviation through the thick glass sample. To estimate the thickness of the poled region, the following equation was used to fit to one peak in the data in Fig. 1, assuming Kleinman symmetry:³

$$P_{2\omega} \propto d_{33}'^2 \sin^2 \theta_{\omega} t_{\omega}^4 T_{2\omega}^2 \Gamma^2, \quad (1)$$

where $\Gamma = \sin[2\pi L(n_{\omega} \cos \theta'_{\omega} - n_{2\omega} \cos \theta'_{2\omega})/\lambda]$, and t_{ω} and

$T_{2\omega}$ are the transmission factors for the front face and the exit face of the sample, respectively. θ_{ω} is the external angle of incidence at the input face, while θ'_{ω} and $\theta'_{2\omega}$ are the internal angles causing walk off. The thickness of the poled region L was found to be 25 μm, much larger than the 5–10 μm already reported.^{1,2} By comparing the harmonic signal generated from a quartz sample (d_{11} , rotation around *z* axis, *x*-input polarization, *y* propagating), it was found that d_{33} of the poled fused silica sample was 0.015 pm V⁻¹, a factor of 30 smaller than that reported.² The reason for this small value is under investigation but we suspect that non optimum poling conditions are responsible.

The coherence length of second-harmonic generation was then measured in an unpoled sample by electric-field-induced second-harmonic (EFISH) generation⁵ to establish the periodicity of the poling electrodes. The samples of commercial grade fused silica (Heraeus type BQ) with approximate dimension of 3 mm×15 mm×25 mm were polished so that the faces were parallel and optically flat. Parallel electrodes were placed on the 15 mm×25 mm faces such that the electrodes over hung the input and output 3 mm×25 mm faces in order that the applied electric field remains constant at the air/silica interface, without fringing⁵ (see inset Fig. 2). The assembly was placed on a rotation stage to alter the propagation path length of the input Nd:YAG 1064 nm *Q*-switched beam during measurements. A Pockels cell driver was used to generate truncated 2.756 kV, 20 ns pulses at 10 Hz across the silica sample, synchronized with the

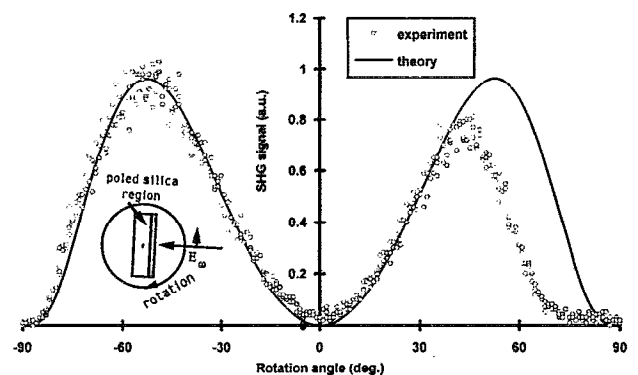


FIG. 1. Second harmonic signal from a 6-mm-thick sample of poled fused silica as a function of rotation angle. The theoretical fit is also plotted.

^{a)}Permanent address: Department of Applied Physics, University of Twente, Enschede, The Netherlands.

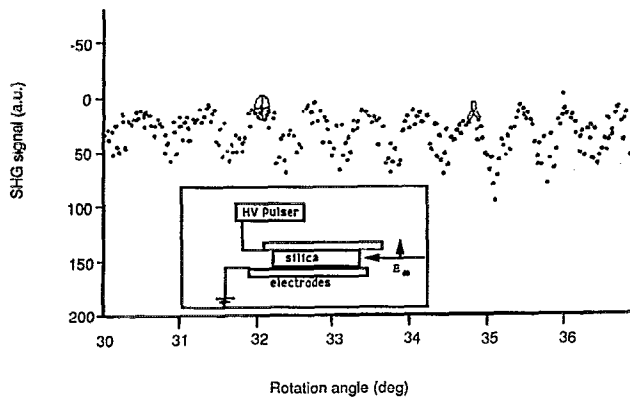


FIG. 2. Electric field-induced second-harmonic generation from a sample of fused silica. The minima at the marked angles were used in the calculation of the coherence length in the design of the periodic electrodes.

arrival of the 10 ns optical pulses. The second-harmonic generation was detected by a photomultiplier tube and displayed on an EG&G Boxcar integrator. The fringes generated as the sample was rotated are shown in Fig. 2. To calculate the refractive index at 2ω , two minima separated by four periods of the Maker fringes between the angles of 32.07° and 34.85° were used, equating Γ to zero, and the following set of equations solved:

$$(n+4)\pi = 2\pi L(n_\omega \cos \theta'_\omega - n_{2\omega} \cos \theta'_{2\omega})/\lambda, \quad (2)$$

$$n\pi = 2\pi L(n_\omega \cos \theta''_\omega - n_{2\omega} \cos \theta''_{2\omega})/\lambda. \quad (3)$$

Using the measured values of the length of the sample, $L=14.133 \text{ nm}$, $n_\omega=1.44963$ and by varying $n_{2\omega}$ around 1.46071, Eqs. (2) and (3) could be solved for $n_{2\omega}=1.45811$. The coherence length calculated from this index was and found to be $23.5 \mu\text{m}$.

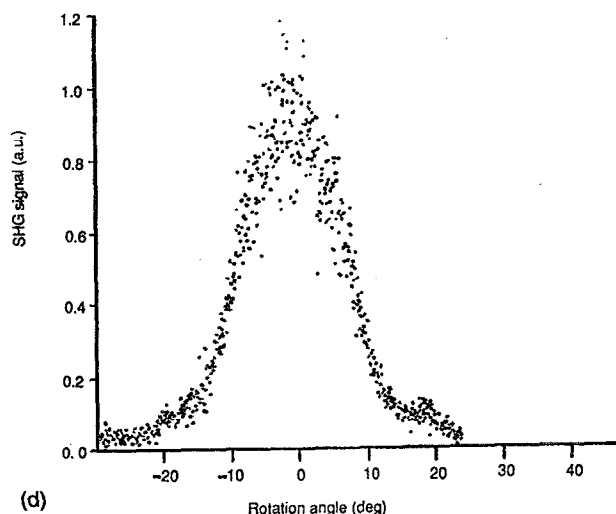
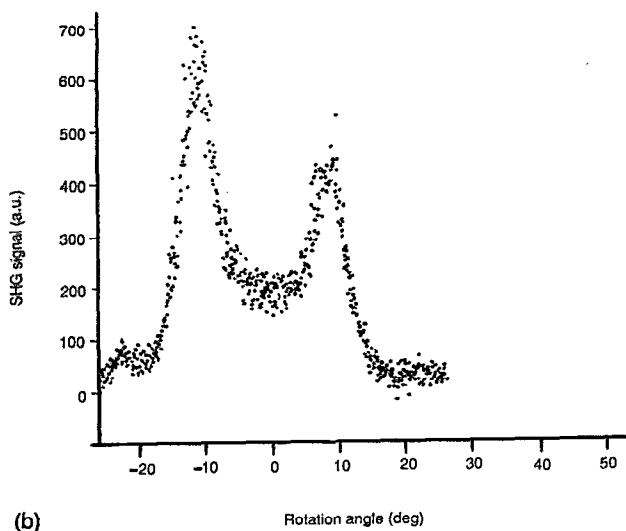
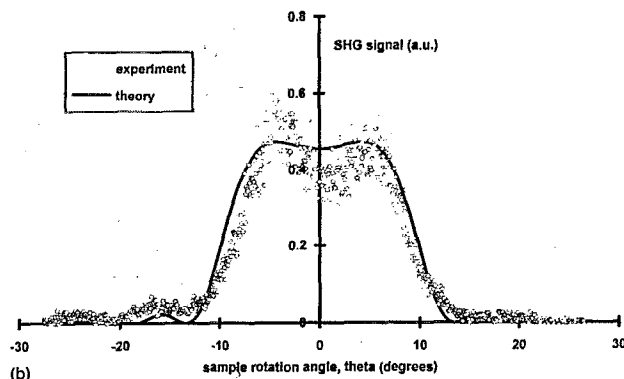
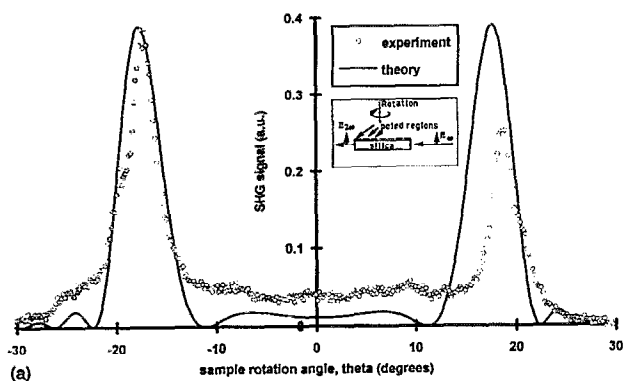


FIG. 3. (a) Phase matching (PM) curve for a poled sample with a period of $47 \mu\text{m}$. The curve fit was done using Eq. (4). Polarization of input beam was parallel to poling direction. (b) PM curve as the period is increased to $47.8 \mu\text{m}$. Note the peaks getting closer to normal incidence, as well as broader. (c) PM curve for a period of $48 \mu\text{m}$, including theoretical fit. The two peaks merge at normal incidence to give a broad saddle response. (d) Near perfect 90° PM. Period of poling used here was $48.2 \mu\text{m}$, giving a broad phase-matching curve.

Since only a single direction of the nonlinearity may be induced easily in the glass close to the anode electrical poling,¹ periodic poling could only be carried out over half the coherence length using our poling technique. A chromium electrode mask was designed with thirteen 10 mm×10 mm regions separated by 1 mm, each with a staggered period, Λ , ranging from 45.8 to 48.2 μm ($\sim 2l_c$) in steps of 0.2 μm , with a mark to space ratio of $\sim 1:11$. This was chosen in an effort to minimize the effects of the fundamental spatial frequency of the electric field spreading at around 25 μm below the surface of the sample.² The pitches were chosen such that an angular rotation of 5° would overlap with the pitch of the next sample. Each periodic electrode was connected by a thin contact to a central pad enabling simultaneous poling of all electroded regions. This mask was then photolithographed onto the central region of a 3-in.-diam polished silica sample $\sim 3\text{-mm}$ -thick evaporation coated with chromium. Standard wet-etching technique was used to produce a replica of the electroded pattern on the sample. The sample was then poled at 5 kV at a temperature of 250 °C for 120 min.

The disk was then cut into thirteen 10 mm×10 mm pieces, optically polished, and the electrodes removed by wet chemical etching. Samples were selected and mounted on a rotation stage such that the focused, or unfocused but apertured beam entered the 3 mm×5 mm face and propagated normal to the electrodes [see Fig. 3(a) inset]. The height of the sample was carefully adjusted so as to maximize the SH signal. The samples were then rotated in turn to produce the phase-matched SH shown in Figs. 3(a)–3(d). Theoretical curves were again used successfully to fit the phase-matching peaks. It may be seen that the bandwidth scales with the angle of incidence with the widest bandwidth for near 90° incidence. As the period deviates from this condition [Figs. 3(a)–3(c)] twin peaks are observed around normal incidence, moving apart with greater phase mismatch, as expected. The asymmetry is due to aperturing effects in the measurements setup. The structure around the central peak becomes apparent only when unfocused beams are used, characteristic of good phase matching.⁵ The angular dependence of the normalized SHG power was modeled using the following relationship:

$$P_{2\omega} \propto k^2 P_{\omega}^2 L^2 \text{sinc}^2(\Delta\beta L/2), \quad (4)$$

with $\Delta\beta = 2\pi[2(n_{2\omega} \cos(\theta_{2\omega} - \theta) - n_{\omega}) - \cos \theta_{\omega}/\Lambda]$. Here P_{ω} is the fundamental wavelength power, k includes the overlap integral between the nonlinear region and the spot size at ω and 2ω , and Fourier coefficient of the fundamental spatial harmonic of the induced nonlinearity.⁵ L is the effective in-

teraction length and Λ is the period of the poling mask. The agreement with the measurements can be seen to be excellent. From the curve fitting, it was deduced that the phase matched length varied between approximately 3.8 to 4.26 mm, i.e., (between 75–85 periods), rather than the 10 mm poled region. The reasons for this is not fully clear, but it is suspected that the angle of incidence of the input beam may not have been normal to the input face, thus traversing the thin poled region at an angle, shortening the interaction length. 90° phase matching was observed in a sample with a period of 48.06 μm , in reasonable agreement with the EFISH measured value of 47 μm .

The peak SH signal from the phase-matched samples was compared with a uniformly poled sample in the same configuration to estimate the effective nonlinearity including the Fourier coefficient. This was found to be 0.05, indicating nonoptimum modulation of the nonlinearity. Further improvements would be necessary in electrode design to allow better efficiencies for device fabrication. Reverse poling to produce alternating regions of $+ve$ and $-ve$ nonlinear coefficient would also improve the SH efficiency fourfold. The estimated effective nonlinearity of the periodically poled sample was $d_{11}/200$ of quartz. However, our uniformly poled samples showed a low nonlinearity to begin with, so that considerable improvement is possible. We estimate that with a nonlinearity of 1 pm/V² and phase matching over the full 10 mm within a waveguide would improve the second-harmonic conversion by a factor of 10⁷, allowing efficient frequency doubling at low powers. These measurements are encouraging for direct periodic poling with e beams on electroded glass samples.

In conclusion, it has been demonstrated that periodic electrical poling for first order nonlinear interaction for second-harmonic generation in fused silica is possible. However, improvements in electrode design and optimisation of poling are necessary before efficient devices can be fabricated.

The authors acknowledge B. J. Ainslie for technical discussions, A. J. Gotts and G. Bickers for cutting and polishing, and R. W. Cecil for assisting with the poling of the silica samples.

¹R. A. Myers, N. Mukherjee, and S. R. J. Brueck, *Opt. Lett.* **16**, 1732 (1991).

²N. Mukherjee, R. A. Myers, and S. R. J. Brueck *J. Opt. Soc. Am. B* (to be published).

³P. G. Kazansky, A. Kamal, and P. St. Russell, *Opt. Lett.* **18**, 693 (1993).

⁴J. Jerphagnon and S. K. Kurtz, *J. Appl. Phys.* **41**, 1667 (1970).

⁵R. Kashyap, *J. Opt. Soc. Am. B* **6**, 313 (1989).